INTERACTION OF SOUND WITH FAST CRACK PROPAGATION : AN EQUATION OF MOTION FOR THE CRACK TIP.

JF. Boudet, S. Ciliberto
Ecole Normale Superieure, Physique Recherche,URA 1325
46 Allée d'Italie
69364 Lyon Cedex 07, France

Novembre 1998

Abstract

The influence of ultrasound on crack dynamics in brittle materials is experimentally studied by using both the natural sound emitted by the propagating crack and an artificially generated ultrasound burst. We show that, although the acoustic energy is much weaker than the energy needed to propagate the crack, the presence of sound waves in the specimen cannot be neglected because sound interacts with the crack tip and may strongly modify the fracture dynamics.
The characterization of this interaction allows us to find an equation of motion describing the crack propagation and the energy balance in mode I.

1 Introduction

Fracture dynamics in brittle materials is a non-linear pattern forming phenomenon, which is not yet very well understood and has been widely studied, both theoretically [1-13] and experimentally [14-23] during the last years, especially in mode I. Recent experiments in Plexiglass and glass have carefully characterized the features of crack propagation [17, 18, 20]. Now, we know experimentally the dependence of the terminal velocity as a function of the relative strain in a finite geometry, but we do not know the equation which determines this dependence. The different instability thresholds, as the appearance of the velocity oscillations, the emission of sound, the roughness

and the micro-branching, are well characterized. But the origin of these instabilities and the link among them are not understood. Clearly, a crack tip equation of motion has not emerged from experimental results.
Another important point is the influence of the sound emitted by the crack on its dynamics. In general, the amount of acoustic energy emitted by the crack is much smaller than the surface energy that one needs to be supplied for the crack to propagate. For example, in PMMA, the maximum acoustic energy is only 5% of the surface energy. However we know from dynamical theory that a small perturbation may produce big changes on the dynamics of an unstable system. Thus the interaction of the crack with sound cannot be neglected in general [21, 24].
The characterization of this interaction allows us to interpret the data in a new way and in particular to try to answer some important questions, such as the equation of motion, the dependence of the surface energy as function of the local velocity and the influence of the geometry on the problem.
The paper is organized as follows : in section 2, we recall the equation of motion found by Dulaney and Brace [12] in 1960. In section 3, the experimental apparatus is described. In section 4, the results on the velocity measurements are reported. In section 5, we present the study of the sound-crack interaction; the experimental set-up, the results and a possible interpretation. In section 6, a new interpretation of the data is reported. Finally, in the appendix, we present a simple model to explain the origin of the velocity instability. This model is mentioned only as a starting point for a discussion.

2 Theoretical approach

The goal of this section is to recall some results established by Mott in 1948 [11] and by Dulaney and Brace in 1960 [12]. By using Mott's calculations, Dulaney and Brace proposed an equation of motion for crack propagation in mode I in an infinite medium. By using this equation, we can show that there is a sound-crack interaction. Therefore we begin by recalling the analysis of Dulaney and Brace.

2.1 The equation of motion for a crack tip

Mott considered the Griffith's energy-balance formulation [25], and he simply incorporated an inertial term E_c into the total energy of a solid with a

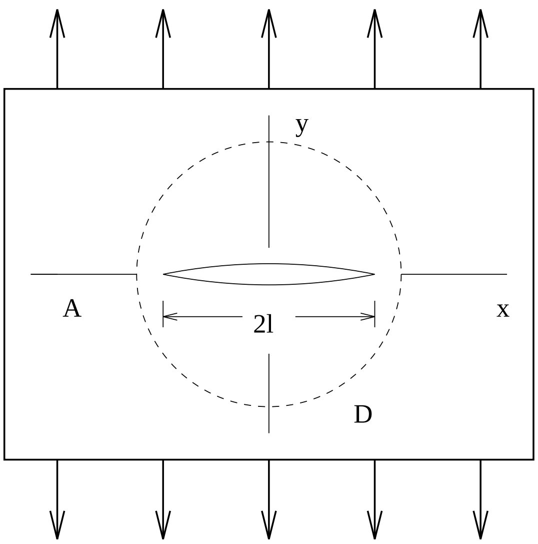

Figure 1: Dynamic plane-crack system. The crack propagates at velocity V. D denotes a domain which receives stress-wave messages from the crack.

straight crack, as shown in Fig. 1. Specifically, he wrote :

$$E_{tot} = E_c + E_p + E_s \ , \tag{1}$$

where E_{tot} is the total energy of the system, E_p is the mechanical energy and E_S is the surface energy of the material. He assumed the following conditions:

i) the stresses and the strains about the moving crack tip are adequately descibed by the equations of static elasticity theory ;

ii) the domain D extends over the entire specimen (if the velocity of the crack is high, then the domain D is unlimited) ;

iii) the fracture surface energy does not depend on the crack velocity.

The second hypothesis allows one to use dimensional analysis and to write an equation of energy-balance. Moreover, Dulaney and Brace consider the special case of a crack in uniform tension and at constant-force loading [12]:

$$E_{tot} = \frac{k\rho\sigma_A^2}{2E^2} l^2 V^2 - \frac{\pi\sigma_A^2}{E} l^2 + 4\gamma l \ , \tag{2}$$

where ρ is the material density, σ_A the applied stress, E the Young modulus, l the length of the crack, V the crack tip velocity, γ the surface energy and k a constant. With the initial condition, $V(l = l_c) = 0$, the authors were able to determine the analytic form of the velocity :

$$V(l) = V_d.\left(1 - \frac{l_c}{l}\right), \tag{3}$$

where V_d is a constant of the material. Stroh [26] in 1950 found that V_d is equal to V_R, the Rayleigh wave speed. In fact, for a large crack length, the surface energy term becomes negligible and the integral equation is similar to the wave equation. So the crack propagates at the velocity of a surface wave of the material. Freund [4] in the seventies found this result too. An unlimited domain is also one of his hypotheses.

2.2 The problems

Of course, Eq.3 presents two problems :

- The first is inherent to our system. We know that in finite dimensions the terminal crack velocity is not the Rayleigh wave speed, but depends on the relative strain of the sample [19, 20].

- The second is that Eq.3 is not integrable at $l = l_c$:

$$V_R t = (l - l_c) + \int_{l_c}^{l} \frac{l_c}{l - l_c} dl \cdot \tag{4}$$

The equation diverges at the origin.

These remarks led us to study the experimental velocity data with the following form ; $V \cdot l$ as a function of l. We obtain ;

$$V \cdot l = V_f \cdot (l - l_0), \tag{5}$$

where l_0 is a length smaller than l_c, which allows to integrate Eq.5. The left hand side term is linear with the crack length. A careful experimental test of Eqs.3 and 5 was one of the motivations of this work.

In fact, this equation of motion was already tested in some experiments [23, 27] and the final result of these experiments was to show that Eq.3 is not a good description for crack motion. This discrepancy eventually led to

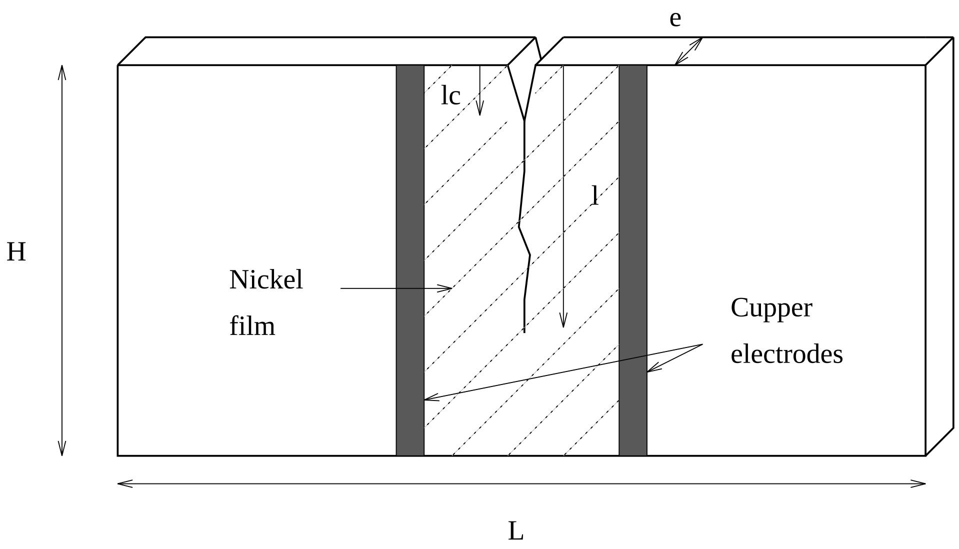

Figure 2: Geometry of the sample. The characteristic lengths are L, H and e.

the current theory of dynamic fracture [4]. However we want to show here that Eq.5 is in agreement with experiments, if the sound-crack interaction is taken into account. The sound-crack interaction masks the underlying equation of motion.

3 Experimental set-up

Experiments have been done using cell-cast Plexiglass (PMMA). The samples have a rectangular shape with a length L of $29cm$ and a height H equal to either 10 or $20cm$. The sample thickness e is varied from $1mm$ to $10mm$, to investigate whether the features of the crack instabilities are independent of the sample thickness. This variation of the thickness concerns only the first part of the results and not the sound-crack interaction. A schematic picture of the geometry of the sample is shown in Fig.2. To induce the fracture just in the center of the sample, an initial cut of length l_c between 5 and $15mm$ was made at $L/2$. Fracture is produced by applying a force in the plane of the sample and parallel to the longest side of the plate (Mode I). The experimental apparatus consists of a tensile machine which can apply a maximum force of about $23000N$. We measure the force F applied to the sample, the crack length $l(t)$ as a function of time and the sound emission produced during the fracture. To measure $l(t)$ we use an improved version of the method described in Ref.[27]. It consists in the measurement of the resistance of a thin conductive film deposited on the surface of the sample. The maximum sensitivity in the measurement of $l(t)$ is better than $0.05mm$ and the absolute accuracy about 5%. The velocity $V(t)$ of the crack is always obtained by taking the derivative of $l(t)$ and the maximum absolute error is below $10m/s$. The sound emission, produced by the moving crack, is measured in the range of 10 kHz-1MHz with several wide band microphones located on the plate surfaces at about 2 cm from the tip of the initial cut. More details about the experimental apparatus can be found in Ref.[20].

4 Results

The goal of this section is not to present all the results, but only to recall some of them which are important to understand the crack dynamics, and specifically the crack tip motion. Before this presentation, it is useful to recall several well established results about crack dynamics, and in particular about the different instabilities. We know that there are two important instabilities in fast crack propagation [14, 17, 18, 20]:

- *The velocity instability :* When the crack reaches a velocity threshold V_{osc} equal to 0.32 V_R, the crack tip begins to oscillate with a typical frequency of $150-300\ kHz$. In the same time, the crack emits acoustic waves at the same frequency and creates micro-cracks in the bulk [17, 20, 21].

- *The roughness instability :* When the crack reaches a velocity threshold V_C equal to 0.45 V_R, its begins to oscillate out-of-plane and generates a roughness on the broken surfaces. The typical wave length of this roughness is equal to 1 or 2 mm [20].

4.1 Macroscopic parameters of crack propagation :

In Fig.3 a typical signal of crack motion is shown, specifically the length of the crack as a function of time for two experiments characterized by a relative strain equal to 2.2 10^{-3} (Fig.3.a) and 5 10^{-3} (Fig.3.b) respectively. With this figure, we can obtain three parameters describing the crack propagation:

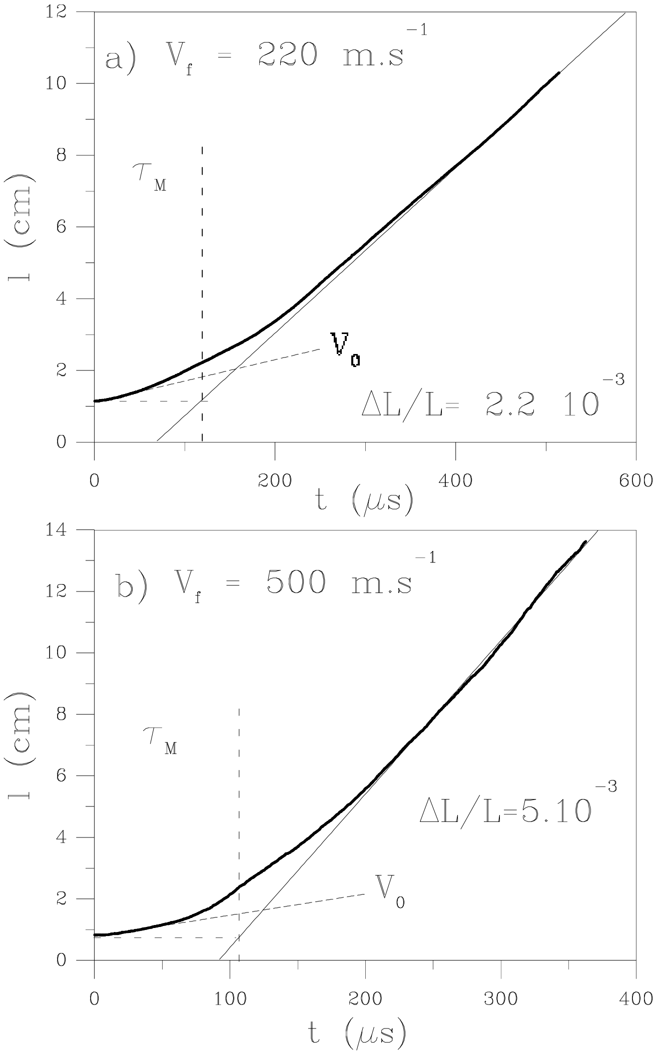

Figure 3: Crack length as function of time for two samples.

1) a non-zero initial velocity V_0, which is the velocity at the beginning of the crack propagation.

2) a velocity plateau, called the final crack velocity, and indicated by V_f.

3) We can also define a third parameter τ_M. By construction, it is the characteristic time of the transient regime. τ_M is the intersection between the asymptote defined by V_f and the line $l = l_c$.

In our experiment, these parameters characterize the crack propagation. We can show that they depend on control and external parameters, specifically the plate geometry, the initial cut and relative strain.

4.1.1 Terminal crack speed :

The first result concerns the terminal velocity. We plot in Fig.4 the crack terminal velocity normalized to the Rayleigh wave speed V_R as a function of the relative strain of the sample. The dotted line is a fit for $(\Delta L/L) > (\Delta L/L)_C$ (see section 5 for details of the fitting procedure). The first result is that terminal crack speed is not the Rayleigh wave speed. The analysis of this curve shows three important points :

(1) the terminal velocity strictly grows with the relative strain;

(2) the terminal velocity domain is in the range of 0.2 V_R-0.7 V_R;

(3) there is a forbidden gap of final speeds between 0.32 V_R and 0.45 V_R. This gap is characterized by a velocity discontinuity, whereas the relative strain is continuous.

These results have two very important consequences:

i) the crack final velocity is imposed by the relative strain.

ii) the gap limits are respectively V_{osc} the velocity threshold for acoustic instability to appear, and V_C the velocity threshold for roughness instability [20].

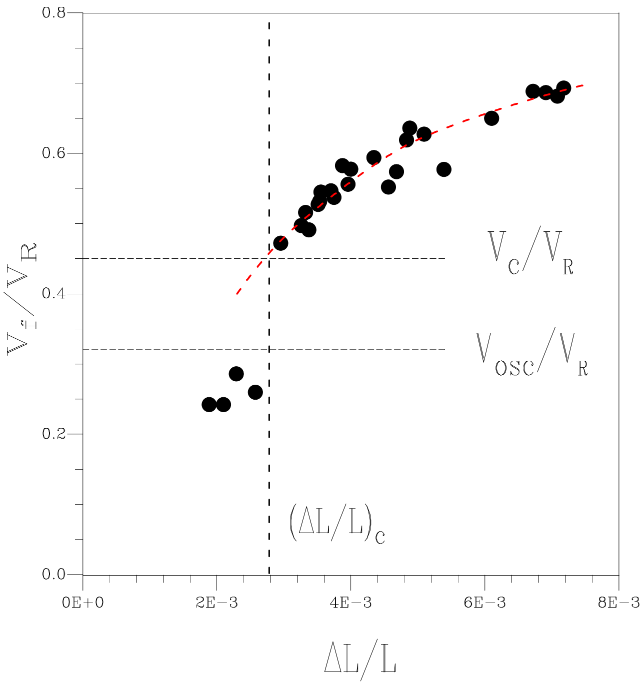

Figure 4: Terminal velocity normalized by the Rayleigh wave speed as a function of the relative strain of the sample. The dotted line is a fit for$(\Delta L/L) > (\Delta L/L)_C$.

4.1.2 Initial Velocity and acceleration :

The characteristic time τ_M is defined in Fig.3. It has been proposed [30] that τ_M can be an useful time to characterize the acceleration phase of the crack. This is the reason why in this section we analyze the behavior of this parameter. We show its dependence on the final velocity in Fig.5.a) and on the initial cut in Fig.5.b). In Fig.5.a, we find once more the transition at V_C, so we may suppose, that at the roughness transition, the crack dynamics is modified. In Fig.5.b, we see the influence of l_c and the appearance of a characteristic length $l_d = 0.8cm$. When $l_c < l_d$, we have a big acceleration and a small characteristic time τ_M. But, when $l_c > l_d$, τ_M stays constant and equal to $150\mu s$. So, we can say that τ_M describes two transitions : the first is the roughness transition, the second concerns the initial cut and gives a characteristic length l_d.

We know since Fineberg's works [17, 18] that, at the level of the experimental resolution, there is an initial velocity jump at the beginning of crack propagation. In figure 6.a, we plot the initial velocity V_0 as function of a velocity constructed from τ_m and l_c. The domain of initial velocity is between $40m.s^{-1}$ and $140m.s^{-1}$, which are similar to Fineberg's observations [17, 18]. Fig.6.a shows that there is a linear dependence between the two velocities V_0 and l_c/τ_M.The higher the initial velocity, the smaller the transient regime. The initial cut influence is not yet well understood; a small initial cut leads to a small initial velocity.

We can use τ_M to define a mean non dimensionnal acceleration A_M:

$$A_M = \frac{V_f/\tau_M}{V_R^2/L}. \tag{6}$$

In Fig.6.b, we show A_M as function of $(\Delta L/l_c)^2$. The mean acceleration grows with $(\Delta L/l_c)^2$, which means that the acceleration depends on the potential energy generated by the strain in the medium, but decreases with the initial cut. The length of the initial cut l_c appears like a length scale for the crack dynamics. More surprising is that when the strain divided by the initial cut goes to zero, the mean acceleration is strictly positive. We have seen that τ_M described two transitions, but in figures concerning the initial velocity and mean acceleration, which contains this time, the transitions disappear. This suggest that l_c presents this transition too.

We present a phenomenological calculation that shows the role of l_c.

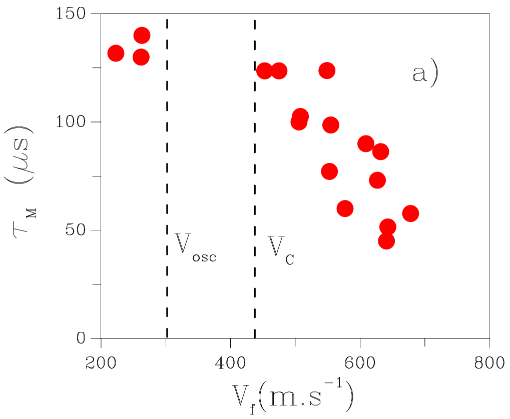

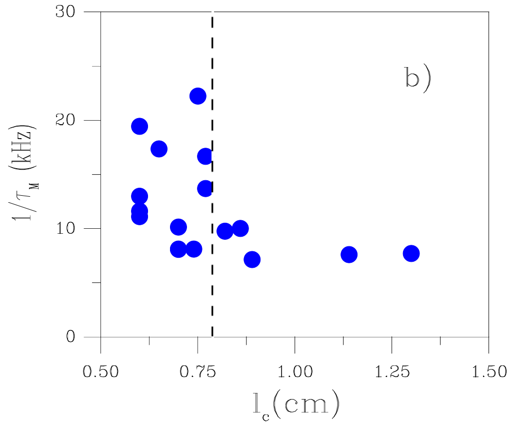

Figure 5: Plots of the characteristic time τ. a) τ_M as a function of V_f. b) τ_M as a function of l_c.

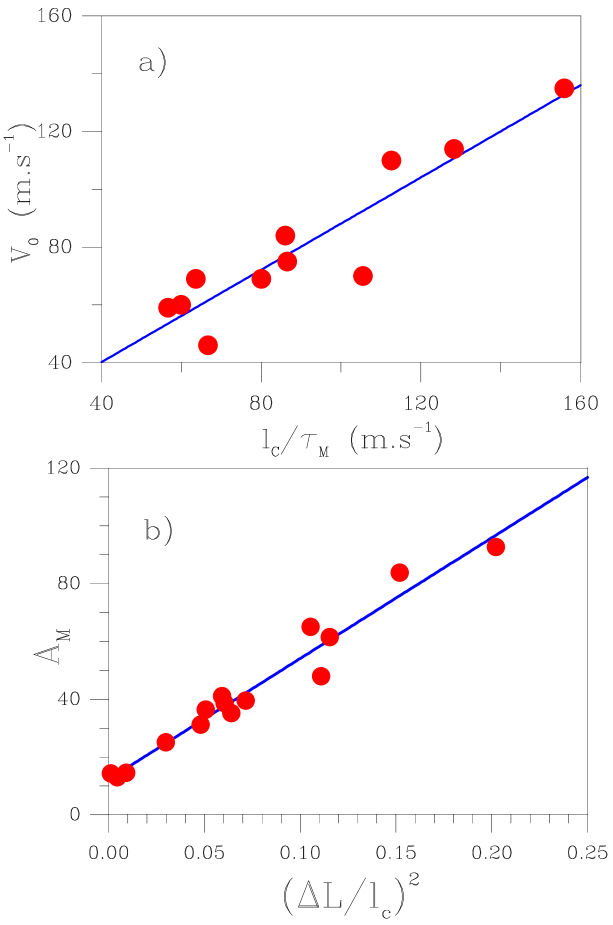

Figure 6: a) V_0 as a function of l_c/τ_M. b) The non dimensional acceleration A_M as a function of the strain normalized by the initial cut.

The idea is to write a "fundamental principle of dynamics", using the dependence:

$$A_M = \frac{V_f/\tau_M}{V_R^2/L} = \alpha \cdot \left(\frac{\Delta L}{l_c}\right)^2, \tag{7}$$

where $\alpha = 420$ is a fitting parameter. Using a force F derived from the potential energy defined in Fq.2, we can obtain a volume force $f(l)$, when we divide by a volume V_e that contains the crack tip:

$$f(l) = -\frac{e}{V_e} \cdot \frac{dE_p}{dl} = \frac{2\pi}{V_e} \cdot \frac{\sigma_A^2}{E'} \cdot le. \tag{8}$$

Moreover, A_M is a mean acceleration, thus we use a mean force and choose $l = L/2$. By substitution in eq.7, we obtain an evaluation of the volume V_e, which can be interpreted as a plastic domain around the crack tip.

$$V_e = \frac{3\pi}{420} \cdot l_c^2 \cdot e. \tag{9}$$

The presence of the thickness is not useful, We can evaluate the surface S around the crack tip; $S = l_c^2/42$. Thus, for $l_c = 6.5mm$, the size of the plastic zone is 1 mm^2, which is not in contradiction with previous estimates (see Barenblatt [31]). Moreover, we see a possible interpretation of the influence of l_c: it is the characteristic length of the plastic zone, created at the moment of the beginning of crack propagation. We suppose, that the plastic zone is not deformed by this propagation.

In conclusion, we see that we can relate the parameters describing the crack propagation with the control parameters. This suggests a functional form of the local velocity of the crack, because the characterization of the mean velocity can be linked to the control parameters. Thus we analyze the local velocity in the following section.

4.2 Local analysis of the velocity

In Fig.7, we show the data of the crack speed for two samples. The first (Fig7 a & c) is a slow crack, i.e. the final speed is below V_{osc}, and the second is a fast crack (Fig7 b & d), where the crack terminal speed is bigger than the threshold for the appearence of velocity oscillations. The signals are presented in two ways, $V \cdot l$ as function of l and V as function of l.

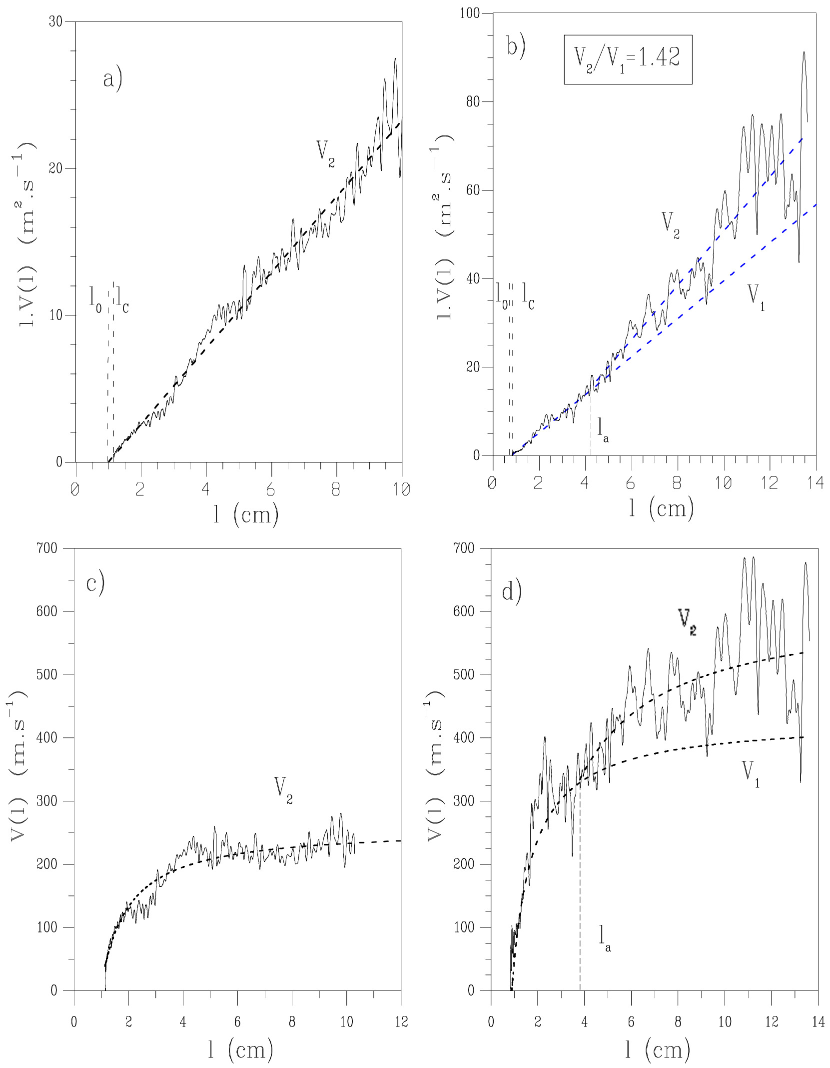

Figure 7: a) and b) $l \cdot V(l)$ as a function of l for a slow crack and a fast crack respectively. c) and d) the corresponding velocity signals as functions of the crack length.

4.2.1 Slow cracks

Looking at Fig7 a & b, we immediately see, that the respective behaviors are different. For the slow crack, there is a linear dependence between $V \cdot l$ and l, and the slope is the crack asymptotic velocity V_2. We can see that the fit (continuous straight line in Fig.7.a) cuts the abscissa axis at $l_0 < l_c$. This behavior is reproducible, and all the slow cracks (i.e. when the asymptotic speed is below V_{osc}) present the following common characteristics:

- a linear dependence between $V \cdot l$ and l,
- a length l_0 smaller than l_c.
- the asymptotic velocity V_2 is equal to the terminal speed V_f.

Thus, the following functional form is a good description of the local crack velocity for slow cracks :

$$V(l) = V_2 \cdot \left(1 - \frac{l_0}{l}\right). \tag{10}$$

In Fig.7.c, we have plotted this functional from with the parameters l_0 and V_2 taken from Fig.7.a, and the agreement is quite good if we neglect the presence of a slow oscillation ($4\ kHz$), which is a resonant frequency of the plate.

4.2.2 Fast cracks

For fast samples (b&d), the functional form is different. In fact, the behavior is linear with two parts. We can define a velocity V_1, which is the asymptotic velocity of the first part, and an adequate length $l_0 < l_c$. Equivalent parameters may be defined for the second part, the asymptotic velocity V_2, which is the terminal velocity, and a length l_1, not reported in the figure, which is the intersection between the fit and the axis. We can also define a length l_a which is the point where the crack changes behavior. This behavior observed in fast cracks with two linear parts in the $V \cdot l$ plot is reproducible. We can always define the following parameters:

- the linear dependence between $V \cdot l$ and l associated with:
- two characteristic lengths, $l_0 < l_c$ and l_a. At l_a the velocity changes and this happens always $80 - 100\ \mu s$ after the beginning of the velocity oscillations,

- two asymptotic velocities V_1 and V_2, whose ratio is always constant and equal to:

$$\frac{V_2}{V_1} = 1.37 \pm 0.05. \tag{11}$$

These results show that the following functional form is a good description of the velocity for fast cracks :

$$V(l) = \begin{cases} V_1 & \cdot \left(1 - \frac{l_0}{l}\right) \text{for } l < l_a \\ V_2 & \cdot \left(1 - \frac{l_1}{l}\right) \text{for } l > l_a \end{cases}, \tag{12}$$

where V_1, V_2, l_0 and l_a are shown in Fig.7.b. The length l_1 is introduced in order to have continuity of the signal, and we have also $V_2 = 1.37\ V_1$. So, if we know l_0, V_1 and l_a, the velocity signal is totally determined. We present this function on the same figure of the velocity signal. We observe a good agreement for the second part, and the difference for the first part starts at the moment where the crack velocity begins to oscillate (at $V(l) = V_{osc}$). This means that velocity fluctuations modify a little the mean velocity behavior.

The Dulaney and Brace analysis seems to be a good description of the crack speed. However when we consider a finite geometry, the terminal velocity is not the Rayleigh wave speed, but it depends on initial conditions, specifically on the plate length and on the relative displacement of the sample.

4.2.3 Analytical formulation of the velocity

For the slow cracks, we can see the agreement in the following way: we can integrate Eq.10 with adequate parameters l_0, V_2, to obtain the evaluation of a computed time t as a function of l', that is :

$$V_2 \cdot t = (l' - l_c) + l_0 \cdot \ln\left(\frac{l' - l_c}{l' - l_0}\right). \tag{13}$$

We see that the initial divergence at $l = l_c$ disappears because the length l_0 is smaller than l_c. We use this artificial way to present the data, because we can not invert Eq.13. The measured crack length $l(t)$ is compared in

Fig.8.a) with $l'(t)$ obtained from Eq.13. In Fig.8.b, the difference between the measured and computed length

$$\delta l = l'(t) - l(t) \tag{14}$$

is presented as a function of time. Both figures show an excellent agreement between computed and measured data, except for the presence of a slow oscillation ($4\ kHz$). This oscillation is a resonant frequency of the plate and its presence has been predicted by Lund [8].
The second element of this analysis is the question of the length l_0. Equation 10 gives at $l = l_c$ an initial velocity which is different from zero ;

$$V_0 = V(l = l_c) = V_2 \cdot (1 - l_0/l_c). \tag{15}$$

This equation introduces a link between the length l_0 and the crack initial velocity V_0. Now, we know that there is a velocity jump at the beginning of the crack propagation. We have introduced l_0 in the integral (Eq.13) of the Dulaney and Brace formula, and the consequence is an initial velocity different from zero. In fact, it is difficult to measure precisely the length l_0 in Fig.7, but the measure of V_0, the velocity jump, is easy. So the parameters introduced in the equation are the terminal velocity and an initial length, the first is related to the relative strain, and the second is determined by the initial velocity jump. Both parameters are sufficient to describe the local velocity as function of the crack length.

4.2.4 Discussion

The main remark is of course, that there is a simple description of velocity data for slow cracks. This analysis seems to be correct for fast cracks, except that the functional form proposed is split into two parts.

There is also an interesting result concerning the length l_a, where the asymptotic behavior of the velocity changes for fast cracks. This change occurs in all the samples around $100\mu s$ after the beginning of velocity oscillations and of acoustic emissions. The interval of $100\mu s$ is exactly the time needed by the acoustic signal to go from the crack tip to the border of the sample and to come back to the crack tip.
This remark leads us to imagine a possible interaction between ultrasound and crack tip. The consequence of this interaction is a change of the asymptotic crack velocity.

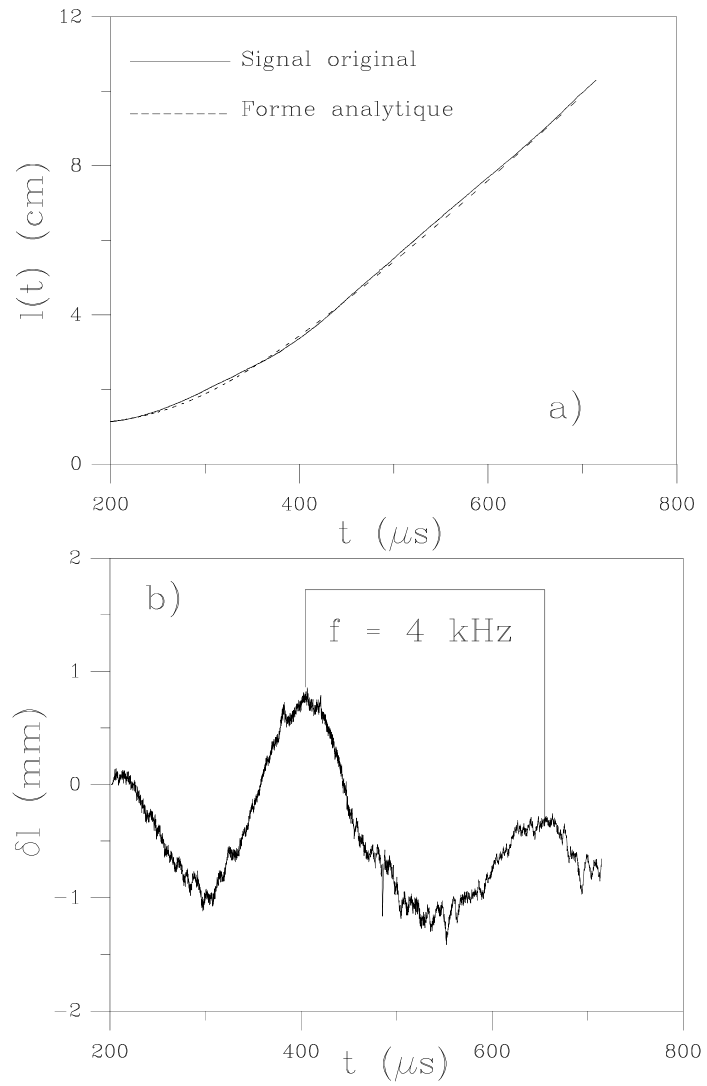

Figure 8: Comparison between experimental data and the analytical function proposed by Dulaney and Brace for a slow crack. a) The continuous line corresponds to the experimental data. The dashed line is the function defined by Eq.13. b) The difference between the two signals presented in a).

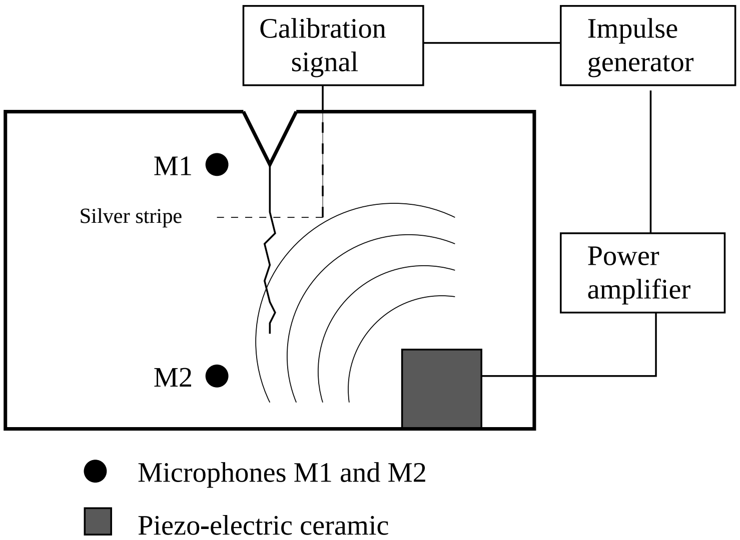

Figure 9: Experimental set-up.

5 Interaction between sound and fracture : experiments, results and interpretation.

To show the link between acoustic emission and the change of the mean crack speed, we have carried out an experiment, whose principle is to perturb the crack growth with ultrasound emitted by a piezoceramic.

5.1 Experimental apparatus

A schematic drawing of the experiment is described in Fig.9. A piezoceramic is mounted on the sample. The piezo-ceramic is driven by a power amplifier whose input is connected to a burst generator. The amplitude and the frequency of this artificially generated ultrasound burst (AGUB) are comparable with those of the natural acoustic emission of cracks. This perturbation experiment is performed in the following way. When the crack, propagating with a constant velocity (which always occurs for $l > 4cm$), arrives at $l \simeq 5cm$, the burst generator is triggered. The generator signal is amplified and sent to the piezoceramic, which emits the AGUB. This sound burst reaches the crack tip $40\mu s$ later, when the crack tip is already at $l \simeq 7cm$. The amplitude of the AGUB is comparable to the natural sound crack emission.

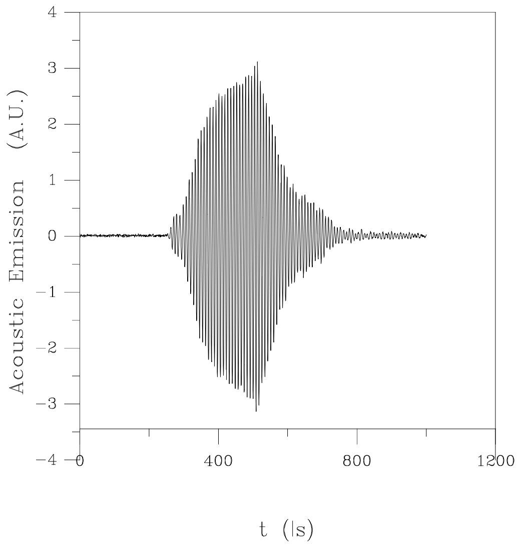

Figure 10: Typical AGUB. The unities are arbitrary. The frequency is equal to 160 kHz.

The AGUB is a burst of 25 cycles at a frequency of 160 KHz or 100 kHz. Notice that the typical frequencies of the natural acoustic emission of a fast crack are between $150kHz$ and $300kHz$. For a plate thickness equal to $4mm$, the corresponding frequency used was 160 kHz, and for a $6mm$ thickness, the corresponding frequency used was 100 kHz. Because of the reflections of the AGUB on the edges of the samples, the crack is in interaction with sound until the final break of the plate. This effect is clearly seen in Fig.10 where a typical AGUB is detected by the microphone M_1 shown in Fig.9. In Ref. [20], we have already shown that the length and the shape of the initial cut determines the final crack speed. Thus we may choose to send the AGUB either on a slow crack, with $V_f < V_{osc}$, or on a fast crack with $V_f > V_{osc}$.

We recall that for $V_f < V_{osc}$ the crack does not produce a continuous sound emission, so the only sound present in the plate is that generated by the piezoceramic.

5.2 Results

5.2.1 Details of one experiment

In Figure 11, we find the typical behaviors of two cracks which have been perturbed in the way described in the previous section. The ultrasound is emitted when the crack is in l_1 and reaches the crack tip when it is in l_2. In Fig.11.a)& c), we have plotted velocity versus crack length for two samples. The corresponding representations in a graph $V \cdot l$ versus l are shown in Fig.11b)& d).

The first sample a) and b) has been broken at a relative strain of $2.3\,10^{-3}$. The final crack velocity without perturbation should be $250\, m.s^{-1} = 0.27\, V_R$, which is below V_{osc}. The second sample c) and d) has been broken at a strain of $5\,10^{-3}$ and the final crack speed should be equal to $560\ m.s^{-1} = 0.59\ V_R$.

In the figure concerning the slow crack, we observe very clearly that the mean velocity changes from $V_1 = 250\ m.s^{-1}$ to $V_2 = 330\ m.s^{-1}$, exactly at the moment where the AGUB arrives. The ratio between the two velocities is :

$$\frac{V_2}{V_1} = 1.35 \cdot \tag{16}$$

This change occurs exactly at the moment where AGUB reaches the crack tip. Finally, we can notice that in this experiment the terminal velocity is in the forbidden gap :

$$V_{osc} < V_2 = 0.37 V_R < V_C \cdot \tag{17}$$

In the figures concerning fast crack, we do not observe a velocity change when ultra-sounds reach the crack tip at l_2. Indeed in this sample the change in velocity has already taken place when the crack tip interacts with its own induced acoustic emission.

5.2.2 Results

To characterize the interaction between sound and fracture, we have changed the characteristic amplitude A of the AGUB, and its frequency too. The main results are the following:

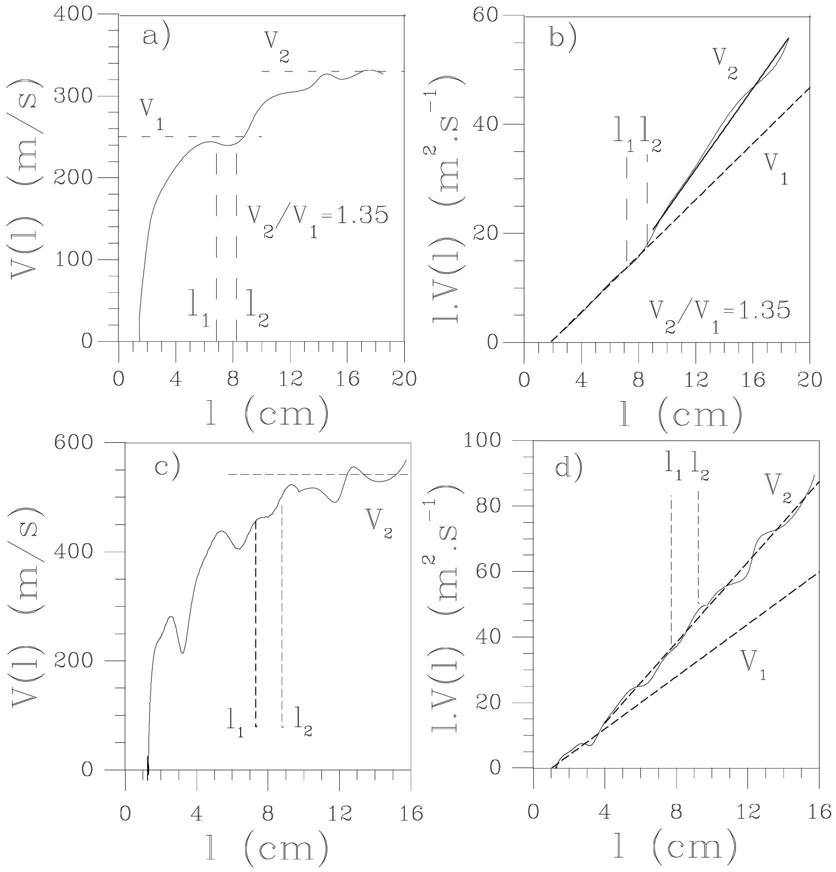

Figure 11: Experiments on sound-crack interaction, in the case of a slow crack a) & b): a) in a standard representation, b) in the representation $V \cdot l$ as function of l. Equivalent figures are shown in figs c) & d) for a fast crack.

a) For slow cracks, the acoustic emission produced by the generator allows us to reproduce the velocity change observed in fast cracks, whose propagation is perturbed by the sound naturally produced by the crack tip. The ratio $R = \frac{V_2}{V_1}$ does not depend on the AGUB amplitude, but may slightly depend on the AGUB frequency.

b) This experiment allows us to produce final velocities in the forbidden gap.

c) There is a threshold A_C. A minimal amplitude is needed to change the crack mean velocity. But, when the signal has an amplitude bigger than A_C, the ratio R does not depend on A. For a frequency of $160kHz$, this threshold is equal to :

$$A_C = 10 \pm 5 \ W.cm^{-2} \ , \tag{18}$$

which represents 0.5% of the surface energy needed to break down the sample. When $A < A_C$, there is no velocity change. For measurements done at a frequency of $100kHz$, the threshold is not yet characterized. The value of A_C measured by means of the AGUB is compatible within error bars with the minimum amplitude of naturally emitted sound detected in our experiment during fast crack propagation. This means that a crack with a terminal velocity equal to V_{osc} emits a signal with an amplitude equal to A_C.

d) The previous points do not apply to a fast crack. The presence of the AGUB does not influence the mean velocity.

e) The sound frequency has an influence on results. We have tested two frequencies ($100kHz$ and $160kHz$) and we obtain the following results which are quite reproducible. At $100kHz$, there is a change of behavior for a slow crack, but R is equal to 1.2 in this case. To summarize, we have :

- For $f = 100kHz$, $R(f) = 1.2 \pm 0.03$
- For $f = 160kHz$, $R(f) = 1.37 \pm 0.05$
- For fast cracks, the frequency of natural acoustic emission f is between $150kHz$ and $300kHz$, and $R(f) = 1.37 \pm 0.05$.

Items c) and d) seem to exclude the possibility of energetic transfer between the acoustic signal and the crack tip. To summarize, the acoustic emission produced by the crack or generated by the piezo-ceramic changes the mean crack speed. This change of mean velocity is not affected by acoustic amplitude (if $A > A_c$) and it does not depend on the sound frequency when $f > 150KHz$.

5.3 Interpretation

Influence of Young Modulus : The important point which relates all these results is the following : PMMA is a viscoelastic material. Therefore, the Young modulus depends on the frequency at which it is measured. The Poisson coefficient stays constant. At high frequencies, we measured the longitudinal and transverse wave speeds, C_l and C_t. These speeds are constant between $200kHz$ and $10MHz$, and equal to:

$$C_l = 2800m/s, \qquad C_t = 1400m/s. \tag{19}$$

These data give a Young modulus equal to $E_d = 6.10^9 N.m^{-2}$. We can thus calculate the Rayleigh wave speed at high frequency :

$$V_R^d = 1300m.s^{-1}. \tag{20}$$

On the other hand, we can also measure the Young Modulus and the Poisson coefficient at low frequency :

$$E_s = 3.2\,10^9 N.m^{-2}, \qquad \nu = 0.33. \tag{21}$$

These determines a Rayleigh wave speed at low frequency :

$$V_R^s = 950m.s^{-1}. \tag{22}$$

We have of course :

$$\frac{V_R^d}{V_R^s} = 1.37. \tag{23}$$

Until now, in order to normalize our results, we used the Rayleigh wave speed and the Young modulus measured statically : E_s and V_R^s.

Imagined process : PMMA viscoelasticity suggests the following process: when the crack velocity is less than V_{osc}, the crack propagates in a medium with an elastic constant E_s. But, when crack reaches V_{osc}, there is a continuous acoustic emission which reflects on the border and comes back to the crack tip. Because of the presence of high frequency oscillations, the relevant elastic constant of the medium where the crack is embedded, is not E_s but E_d. Therefore, the crack tip accelerates to reach a new final velocity V_2 compatible with the applied strain and the new Rayleigh wave speed V_R^d. We can thus define an effective Rayleigh wave speed, which is the Rayleigh wave speed really "seen" by the crack tip :

$$V_R^* = \begin{cases} V_R^s & \text{when } V(t) < V_{osc} \\ V_R^d & \text{when } V(t) > V_{osc} \end{cases} . \tag{24}$$

Specifically we can say that the strain $\Delta L/L$ determines a first final velocity:

$$V_1 = V_R^s.g(\Delta L/L), \tag{25}$$

where g is an increasing and continuous function of the relative strain. Now, if V_1 is smaller than V_{osc}, there is no crack-sound interaction, so $V_R^* = V_R^s$ and the observed final velocity is really V_1. In contrast for a fast crack, sound perturbs the crack dynamics and the effective Rayleigh wave speed is now V_R^d and the new terminal velocity becomes :

$$V_2 = V_1.\frac{V_R^d}{V_R^s} = 1.37V_1. \tag{26}$$

The function $g(\Delta L/L, L)$ is a relationship between the terminal velocity and the relative strain when V_R^d is equal to V_R^s, that is the material is perfectly elastic. This function can be determined from the experimental data since we know the final velocity as a function of $\Delta L/L$ (see Fig.4).

6 A new interpretation of the results

6.1 Final velocity

To find g, we have just to plot V_f/V_R^* as a function of $(\Delta L/L)$. We can see the results in Figure 12.

We see that g is always an increasing and now continuous function of $\Delta L/L$.

We can redefine the terminal velocity domain :

$$0.2\ V_R^* < V_f < 0.5\ V_R^*. \tag{27}$$

The different thresholds of instabilities change too:

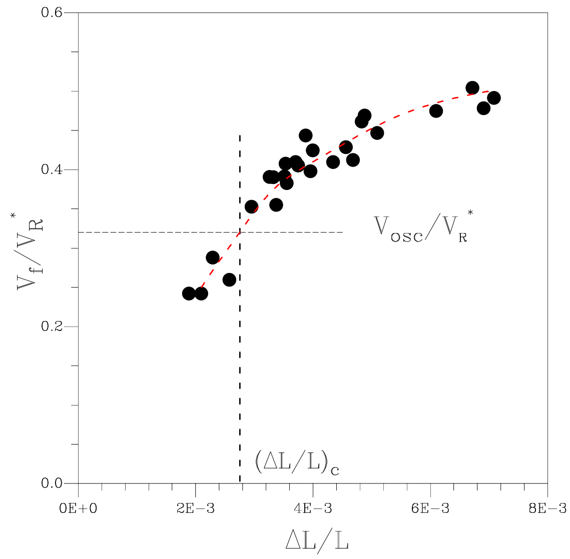

Figure 12: This figure is equivalent to Fig.4 except that we use the effective Rayleigh wave speed V_R^* as a normalization factor of V_f.

velocity instability threshold: $V_{osc} = 0.33V_R^*$,

roughness instability threshold: $V_C = 0.33V_R^*$,

macro-branching instability threshold: $V_b = 0.5V_R^*$,

We notice immediately that the first two thresholds occur at the same value:

$$\frac{V_{osc}}{V_R^*} = \frac{V_C}{V_R^*}, \tag{28}$$

although $V_C = 1.37V_{osc}$. This remark is very interesting, because it suggests a link between the two instabilities. Indeed, the tip of a fast crack crosses two times the same threshold instability. The first time, it generates a velocity instability and an acoustic emission. When it crosses for the second time the instability, then the sound-crack interaction seems to generate the roughness instability. So we can write:

When the crack tip crosses the first instability, there is no roughness, the crack tip oscillates in the crack plane. We can call it *a longitudinal instability* of the crack tip.

When the crack crosses the second instability, the crack tip begins to oscillate out of plane, because of the appearance of roughness. We can then speak of *a transverse instability* of the crack tip.

Moreover, it is interesting to notice that experiments on fracture done in different materials such as steel and glass lead to the common conclusion that velocity oscillations generate roughness oscillations. The reason is that in these materials the thresholds are the same, since in glass and steel, the viscoelastic effect is very small. Indeed, the dynamical and the static Young modulus differ by a few percentage points. This explains also why the forbidden gap is too small to be detected in these materials.

Finally, we notice that the macro-branching threshold occurs at a value compatible with Yoffe's prediction [28].

6.2 The equation of motion of a crack tip

Using the idea of the existence of an effective Rayleigh wave speed as described in Eq.24, the function proposed by Dulaney and Brace becomes also

a good description for the fast cracks.
We have already seen in section 4 that the following function is a good description of the slow cracks :

$$V(l) = V_f \cdot (1 - l_0/l). \tag{29}$$

We also know that this function is correct for the fast cracks with two terminal velocities : $V_2 = 1.37V_1$. In section 4 we have shown that the transition from V_1 to V_2 occurs because of crack-sound interaction.

In Fig.13, we compare the equation of motion and the data in the same way as in Fig.8 for slow cracks. In Fig.13.a& b, we have reported the velocity data in the representations $(V \cdot l, l)$ and (V, l) respectively. From Fig.13.a we can determine the fitting parameters (l_0, V_1) and l_a the length signaling the beginning of sound-crack interaction. We calculate the velocity in the first part when l is between l_c and l_a ($3.8\ cm$) and with Eq.13 we can compute a time t as function of the crack length l'. We can make the same calculations on the second part, when l is bigger than l_a with the parameters l_2 and V_2 :

$$t = \begin{cases} \frac{1}{V_1} \cdot & \left[(l' - l_c) + l_0 \cdot \ln\left(\frac{l'-l_c}{l'-l_0}\right)\right] \text{for } l' < l_a \\ \frac{1}{V_2} \cdot & \left[(l' - l_c) + l_1 \cdot \ln\left(\frac{l'-l_c}{l'-l_1}\right)\right] \text{for } l' > l_a \end{cases}, \tag{30}$$

Now, we can compare this equation with the data. In Fig.13.c, we have plotted the original data and the signal computed from Eq.30. The agreement is excellent except for the last centimeter. We have plotted the difference between the two signals in Fig.13.d, where δl is given by Eq.14. The difference is below 1 mm, until 13 cm. Like in Fig.8, there is the presence of a resonant frequency of the plate. To conclude, we can say that the agreement is very good.
Moreover, there are just 2 free parameters : l_0 and V_1 obtained by fitting $V(l) \cdot l$. In fact, V_2 is determined by the following equation :

$$V_2 = 1.37\ V_1. \tag{31}$$

The length l_1 is determined by continuity of the velocity and we can calculate l_1 in the following form :

$$l_1 = l_c \cdot \left[1 - \frac{V_R^s}{V_R^d} \cdot (1 - \frac{l_0}{l_c})\right]. \tag{32}$$

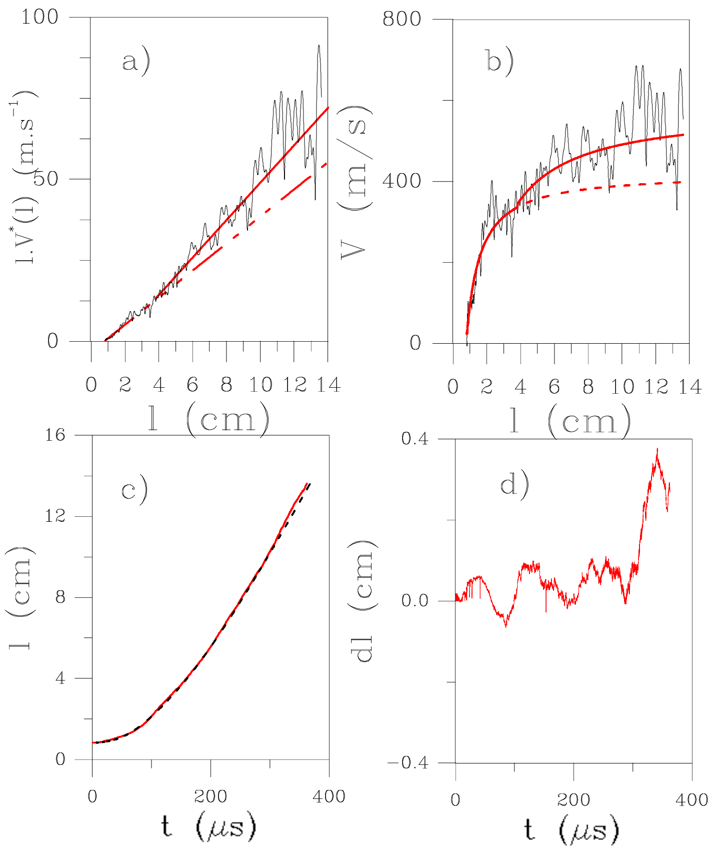

Figure 13: Comparison between Eq.29 (dashed line) and data (continuous line) for a fast crack.

The length l_a is also determined because it corresponds to the time needed by the acoustic wave to go to the borders and to come back. When l is bigger than l_a, there are no free parameters.

Then, we can conclude that Eq.30 with two parameters V_f and l_0 is a very good approximation of the velocity signal. In the case of fast cracks, this was masked by the sound-crack interaction.

6.3 Initial velocity and mean acceleration

Moreover, we see that one can find the initial velocity V_0 as a function of the other parameters:

$$V_0 = V_f \cdot \left(1 - \frac{l_0}{l_c}\right). \tag{33}$$

Experimentally, it is very difficult to measure exactly l_0, especially for the fast cracks. Then, we preferred to construct a length l_0 from the initial velocity in this way:

$$l_0 = l_c \cdot \left(1 - \frac{V_0}{V_f}\right). \tag{34}$$

One can see that this length l_0 is a linear function of l_c. The experimental results are plotted in Fig.14 and we obtain a linear dependence, with a slope equal to 0.7. Then, l_0 is a correction of the initial cut, because $l_c - l_0$ is 30% of l_c. This also means that V_0/V_f is constant. Moreover, l_0 is always smaller than l_c, which permits to integrate the equation of motion over time.

Now we can come back to the problem of the mean acceleration defined in Fig.6. We recall the definition of τ_M, that is:

$$(l - l_c) = V_f \cdot (t - \tau_M). \tag{35}$$

First, the presence of the sound-crack interaction, which modifies the dynamics, implies that τ_M is not relevant. Secondly, if we forget the sound-crack interaction, and if we consider Eq.29 as relevant to describe the crack dynamics, we can try to calculate τ_M. Thus, if we use Eq.35 to define τ_M in substitution of Eq.13, we obtain :

$$\tau_M = t - \frac{l - l_c}{V_f} = \frac{l_0}{V_f} \cdot \ln\left(\frac{l - l_c}{l - l_0}\right). \tag{36}$$

We see immediately that τ_M goes to zero when l becomes infinite. Thus, τ_M and the mean acceleration A_M are not well defined, and are not useful parameters to describe the beginning of crack dynamics.

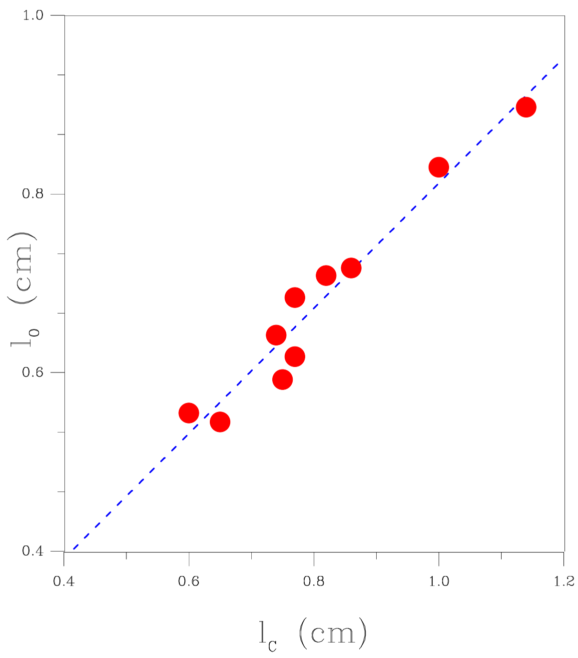

Figure 14: the length l_0 as function of l_c. The dotted line is a fit with a slope equal to 0.7.

6.4 Energy balance

We can now try to find an equation of motion for the crack tip. This is possible by the development of Eq.29 and by identifying the different terms of the potential, the kinetic and the surface energies, respectively E'_p, E'_c and E'_s. We consider the function in Eq.29 as relevant to describe fast crack propagation at constant displacement (when the viscoelastic effect has been already taken into account in the way described in section 6.2). V_f is the terminal velocity in any case. By squaring and developing Eq.29, we obtain:

$$l^2V^2(l) - V_f^2 l^2 + 2V_f^2 l_0 l = l_0^2 V_f^2. \qquad (37)$$

In order to obtain the potential energy, that we know exactly in our configuration ($E' = E/(1-\nu)$), We can multiply this equation by $(\pi\sigma_A^2)/(E'V_f^2)$. So,

$$\frac{\pi\sigma_A^2}{V_f^2 E'} \cdot l^2 V^2 - \frac{\pi\sigma_A^2}{E'} \cdot l^2 + \frac{2\sigma_A^2}{E'} \cdot l_0 l = \frac{\pi\sigma_A^2}{E'} \cdot l_0^2 \qquad (38)$$

The right hand side term in Eq.38 is the total energy and it will be neglected in the following analysis. This representation allows us to find the different energies:

$$\begin{cases} E'_c &= \frac{\pi\sigma_A^2}{V_f^2 E'} \cdot l^2 V^2\,, \\ E'_p &= -\frac{\pi\sigma_A^2}{E'} \cdot l^2\,, \\ E'_s &= \frac{2\sigma_A^2}{E'} \cdot l_0 l\,. \end{cases} \qquad (39)$$

We notice that the terms of the kinetic and the surface energies are very similar to those introduced by Mott.

Kinetic energy : By introducing $V_f = V_R.g(\Delta L/L = \sigma_A/E, L)$ and $V_0 = \sqrt{E/\rho}$, we can write this term in our configuration :

$$E'_c = \frac{\pi\sigma_A^2}{g(\sigma_A/E, L)E'} \cdot \frac{V_0^2}{V_R^2} \cdot l^2 V^2\,. \qquad (40)$$

If we recall the term evaluated by Mott in an infinite medium;

$$E_c = \frac{k'\rho\sigma_A^2}{2E^2} \cdot l^2 V^2\,, \qquad (41)$$

the only difference is the appearance of a coefficient;

$$\frac{1}{g(\sigma/E, L)}. \tag{42}$$

We can write this because we can put $2\pi E'/\rho k' = 1$. Then, the coefficient can be interpreted as a finite size contribution. The correspondence will be complete if we have the following result when L becomes very large:

$$\lim_{L\to\infty} g(\Delta L/L, L) = 1. \tag{43}$$

Surface energy : Mott's expression - $E_s = 4\gamma l$ - is very different from our expression, but we know that if Griffith's criterion [25] is relevant, we can introduce a characteristic stress σ_C, and write;

$$\gamma = \frac{\pi\sigma_C^2}{2E'} \cdot l_c.$$

The terms are then similar except that we have $\sigma_A l_c^{1/2}$ instead of $\sigma_C l_0^{1/2}$. We can say that we replace (σ_C, l_c), which described theoretically the Griffith criterion by (σ_A, l_0), which allows us to integrate the equation of motion, Eq.14. We have chosen to compare the surface energy E'_S with the minimal surface energy γ needed to break the sample. In figure 15, we show this as function of terminal velocity. The continuous line is the common by admitted value of the surface energy ($\gamma = 150 J.m^{-2}$) in PMMA [see [16]].

The data are between γ and 4γ, and the errors are big because of the difficulty to evaluate the length l_0. The results are good for slow cracks, for which the evaluation of l_0 is more precise.

In conclusion, we can say that the conducted analysis does not fall into contradictions in the evaluation of the surface energy. Fig.15 does not allow us to establish definitive statements, but it shows that the value of the surface term obtained by our analysis is close to the commonly accepted one. Furthermore we are unable to conclude whether the surface energy depends on crack velocity. However, there is no need to use a surface energy depending on the local velocity and it seems possible to use a constant value of γ.

To conclude this analysis, we can say that the analytical form of the velocity and of the energy balance is not inconsistent with the theoretical knowledge in an infinite medium. The only difference is the introduction of a dependence of the kinetic energy on the length L. Moreover, it seems

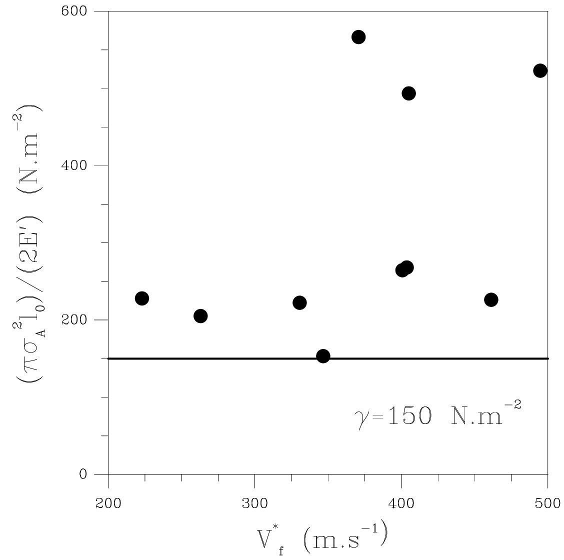

Figure 15: An evaluation of the surface energy $\gamma = \pi\sigma^2 l_0/2E'$ as a function of the effective final velocity defined by $V_f^* = V_f \cdot \frac{V_R}{V_R^*}$.

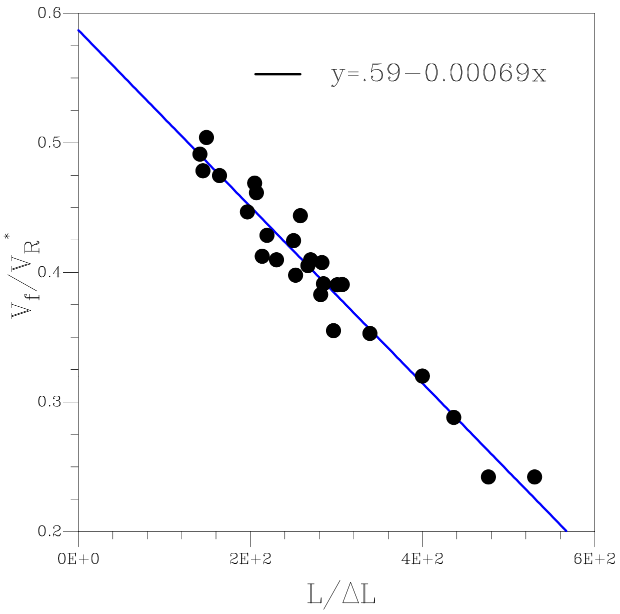

Figure 16: The terminal velocity normalized to the effective Rayleigh wave speed as a function of the relative strain.

possible to analyze experimental data without introducing a surface energy dependent on the velocity [4]. This possibility is rather uncommon and must be pointed out.

6.5 Terminal velocity as function of the relative strain

We can now search for a dependence between the terminal velocity V_f and the relative strain $\Delta L/L$. This is shown in Fig.16.

By using $(L/\Delta L)$, we obtain a linear dependence between the two terms:

$$\frac{V_f}{V_R^*} = \frac{V_L}{V_R^s} \cdot \left[1 - \frac{(\Delta L)_c}{\Delta L}\right] \ , \tag{44}$$

where $V_L = 0.6\ V_R^S$ and $(\Delta L)_c/L = 1.2\ 10^{-3}$. Of course V_L must depend on the length L, since L is the only geometrical parameter which is not varied in our experiment. If

$$\lim_{L\to\infty} V_L(L) = V_R^s, \tag{45}$$

all the predictions would become consistent.

The influence of L: In order to check this prediction, about the dependence of V_L on L, we have varied the length L. In the experiments described in the previous section, L was constant and equal to $25cm$, and only H and e were varied. In this section, we described results obtained in plates with $L = 10cm$ and $17.5cm$. The lengths H and e are constant, equal to 20 cm and 4 mm respectively. If we define the aspect ratio $r = L/H$, we have explored the following domain:

$L = 25cm$: $1.25 < r < 2.5$ (in the previous section).

$L = 17.5cm$: $r = 0.875$.

$L = 10cm$: $r = 0.5$.

In a first approximation, we can say that we have in the first case, $r > 1$; in the second and the third cases, $r < 1$. We know also that in the first case, H or e have no influence on the results. The results are presented in Fig.17, where the terminal velocity V_f normalized to the effective Rayleigh wave speed is shown as function of $L/\Delta L$. The measurements made with other lengths are consistent with the previously described measurements. The existence of a forbidden gap and the sound-fracture interaction are still observed. Since all the results are confirmed, we test the hypothesis :

$$\lim_{L\to\infty} V_L(L) = V_R^s. \tag{46}$$

In Fig.17, we can immediately see that there is still a linear dependence between V_f/V_R^* and $L/\Delta L$, but for the same relative strain the fastest crack occurs in the plate with $r \simeq 1$.
For example, if we consider a final velocity equal to $0.5V_R^*$, we have :

- for $L = 25cm$ and $r > 1$, it needs a relative strain equal to $6.6\,10^{-3}$,

- for $L = 17.5cm$ and $r \simeq 1$, it needs a relative strain equal to $2.5\,10^{-3}$,

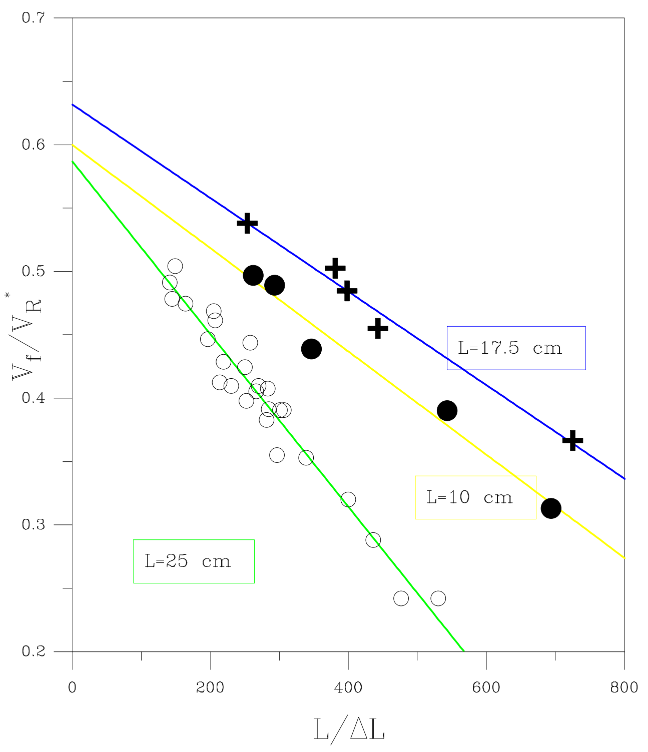

Figure 17: V_f normalized by V_R^* as a function of $L/\Delta L$: the empty circles correspond to $L = 25cm$, the circles to $L = 10cm$ and the crosses to $L = 17.5cm$.

- for $L = 10cm$ and $r < 1$, it needs a relative strain equal to $3.3\,10^{-3}$.

These surprising results lead us to think that the aspect ratio plays an important role in the determination of V_f. As it has no influence for plates of $25cm$, we can conclude, that its influence is felt when $r < 1$. Why $r \simeq 1$ is a transition ? We have seen the influence of an acoustic wave on crack dynamics. Now, $r \simeq 1$ is the limit where an acoustic wave emitted by the crack is first reflected either by the sides of the plates parallel to the crack direction or by the perpendicular ones. Moreover, in the literature [29, 14, 22] this value is also important for the following reason: the aspect ratio has to be bigger than 1 in order to have a crack propagating itself in a medium in acoustic equilibrium.
Extrapolating the fit of the velocity to the point where $(L/\Delta L)$ goes to zero, i.e. at infinite strain, the terminal velocity seems to be relatively constant:

$$\frac{V_f}{V_R^*}\Big(\Delta L \to 0\Big) = 0.61 \pm 0.02\cdot \tag{47}$$

This means that at infinite strain the geometry has no influence on the final velocity. But, in contradiction with Eq.46, the velocity at infinite strain is equal to $0.61\ V_R^S$.
We did not test sufficient lengths L in order to really establish a law for V_f.

6.6 Comparisons with other experiments

The sound-crack interaction is important to understand crack propagation. It allows us to see with new eyes some previous experiments, specifically those performed by *Kerkhof* [23], *Green and Pratt* [22] and *Sharon and Fineberg* [17, 18].

Kerkhof experiment : We quickly recall the main results obtained by Kerkhof in the sixties. The idea is to send a highly energetic high frequency transverse wave into the crack tip during its propagation. The measures of the periodic roughness let him evaluate the local crack tip velocity. The hypothesis is of course that there is no interaction between crack propagation and sound, except a small roughness. The typical frequency used is $500kHz$ in PMMA and $1.5MHz$ in glass, i.e. it is rather close to the one that we use in PMMA. We know now that the hypothesis is not correct. There is an interaction between sound and fracture. Of course, we do not know exactly the amplitude of the sound signal, and secondly, we have not shown that at the frequency used by Kerkhof, there is an interaction. Nevertheless, we can say that the results obtained by Kerkhof must be confirmed.

Green and Pratt experiments : There is in the literature an experiment which is close to our results concerning the sound-crack interaction. It is the one performed by Green and Pratt in PMMA in the seventies. The experiment is similar to ours. They measure mechanical energy balance rate G, and the terminal velocity. G begins to change drastically when the velocity is higher than $450 m/s$; moreover, the crack begins to develop roughness. The authors identified the change of Young modulus with frequency. They gave the values; $E_S = 3.1\, 10^9 N.m^{-2}$ and $E_d = 7.6\, 10^9 N.m^{-2}$ for the static and dynamic modulus respectively. They interpreted the transition at $450 m/s$ as a result of the change of the Young Modulus. With the other data in their article, we can calculate both Rayleigh wave speeds:

$$V_R^s = 935\ m/s\ , \qquad V_R^d = 1450\ m/s\ \cdot$$

The roughness instability occurs at $V_C = 0.31\ V_R^d = 0.48\ V_R^s$. The velocity instability threshold, which they do not know, will occur at $0.31 V_R^s$ too. This experiment is consistent with our measurements, their interpretation needs the introduction of two Young Modulus. Our results justify this introduction, and their results are quantitatively consistent with ours.

Sharon and Fineberg experiments : Their data and ours show a great deal of agreement : the velocity instability, the domain of final velocity, the domain of initial velocity and the behavior of the velocity.
However they never pointed out the existence of a dynamic Young modulus. So we do not know if the sound-crack interaction is detectable in their experiments.
Their experiments concern specifically the appearance of the micro-cracks. The micro-cracks begin to appear with the velocity fluctuations, but it does not seem that the micro-cracks generate the velocity oscillations. The main reason is that the size of the micro-cracks is typically $500\mu m$ and the characteristic size of the velocity fluctuations is $2mm$. It is possible to imagine the following scenario : when the crack velocity reaches V_{osc}, the crack tip begin to oscillate in its propagation plane and generates micro-cracks in the volume which generate the acoustic wave emissions. We may integrate Fineberg's work and ours into a crack description which is not in contradiction. To conclude, it appears useful to study at same time the micro-cracks

and the acoustic emissions in order to discover the origin of the crack velocity oscillations.

7 Conclusions :

We have extended the experimental results of Reference [21] on the sound-crack interaction. The novel features of this investigation are :

1) PMMA is a viscoelastic material: we can define two frequency domains where the elastic data -the Young Modulus, the Poisson coefficient and the wave speeds- are constant. Thus, we can define two Rayleigh wave speeds, called static Rayleigh wave speed for low frequencies and dynamic Rayleigh wave speed for high frequencies. Experimentally, we have shown that both Rayleigh wave speeds are relevant to describe the crack motion, depending on the presence of a high-frequency acoustic wave. This wave is emitted by the crack and interacts with the crack after the reflection on the borders. This interaction has to be incorporated into any description of crack motion. Indeed, this interaction generates a constant terminal velocity jump. The characterization of this interaction allows us to understand several crack properties.

2) The first interesting property is a crack tip equation of motion. We have proven that in our geometry the equation found by Dulaney and Brace is relevant to describe the crack propagation, except for the problem of the limiting velocity and the initial condition. This new equation is:

$$V(l) = V_f \cdot (1 - \frac{l_0}{l}). \tag{48}$$

   All our experiments are described by this equation. The mean speed of slow cracks is controlled directly by this equation. For the fast cracks, we must add the terminal velocity jump due to sound-crack interaction, which masks the underlying equation of motion. This equation is controlled by two free parameters: the terminal velocity V_f and a length l_0 smaller than the initial cut l_c.

3) These free parameters are completely determined by the external control parameters in the following sense: V_f is an increasing function of

strain, and it depends on the length L. We have characterized the dependence of the relative strain when L is constant:

$$V_f = kV_R^* \cdot (1 - \frac{\Delta L_c}{\Delta L}), \tag{49}$$

where k and ΔL_c depend on L.
We have tried to understand the influence of the length L, but the few values of L that were explored are not enough to characterize this dependence. The results found for $L = 25cm$ are observed for the other tested lengths too. We can only say that in order to describe the influence of L, we need to introduce the aspect ratio $r = H/L$ and the preliminary results are not in contradiction with the following assumption :

$$\operatorname*{Lim}_{L \to \infty} V_f = 0.61\ V_R. \tag{50}$$

The length l_0 depends only on the initial cut l_c and it is equal to 0.7 l_c. The origin of this length seems to be the Griffith criterion.

4) The equation of motion allows us to write a phenomenological energy balance. We can find an expression for the kinetic energy from which follows the dependence of the final velocity on the relative strain. We can also define a surface energy γ, whose values are consistent with those measured for PMMA. This surface energy is related to the stress and the length l_0 by an equation identical to the Griffith's criterion. We can say that the parameters l_0 and σ_A are linked between themselves by a static energy balance like Griffith's criterion.
More importantly, we do not use a surface energy depending on the local velocity to write this energy balance.

5) (See appendix) We think that the origin of the velocity instability is a resonance of the crack front in the thickness of the samples. The reasons of this argument are, first of all that the velocity threshold is a constant in two different materials such PMMA and glass. Secondly the frequency of velocity oscillations decreases with the thickness. Moreover, the typical frequencies are compatible with a wave speed divided by the thickness.
We propose a simple model in which the crack front is resonant with the thickness. We find a velocity threshold, above which the crack

begins to oscillate. The value is given by :

$$C_t^2 = V_R^2 + V_{osc}^2 \tag{51}$$

The threshold depends only on Poisson's coefficient which agrees with the experiments. The frequency of velocity oscillations is equal to $V_R/2e$ which is close to what is observed in our experiments.

We wanr to thank Rodrigo Arias to the carrefully reading of the manuscript.

References

[1] 1. Adda-Bedia M. & Ben Amar M. (1997) Morphological instabilities of dynamic fractures in brittle solids. preprint. Voir également, (1996) itshape Phys. Rev. Lett. **76** 1497.

[2] 2. Ching E. (1994) Dynamic stresses at a moving crack tip in a model of fracture porpagation. *Phys. Rev. E* **49** 3382.

[3] 3. Cotterel B. & Rice J.R. (1980) Slightly curved or kinded cracks. *Int. J. Fract.* **16** 155.

[4] 4. Freund L.B. (1990) Dynamical fracture mechanics. Cambridge University Press, New-York.

[5] 5. Kostrov B.V. (1975) On the crack propagation with variable velocity. *Int. J. of Fracture* **11** 47.

[6] 6. Langer J.S. (1992) Models of crack propagation. *Phys. Rev. A* **46** 3123.

[7] 7. Langer J.S. (1993) Dynamical model of the onset and propagation of fracture. *Phys. Rev. Lett.* **70** 3592.

[8] 8. Lund F. (1996) Elastic forces that do not work and the dynamics os fast cracks. *Phys. Rev. Lett.* **76** 2742.

[9] 9. Marder M. (1991) New dynamical equation for cracks. *Phys. Rev. Lett.* **66** 2484.

[10] 10. Marder M. (1993) Simple models of rapid fracture. *Physica D* **66** 125.

[11] 11. Mott N.F. (1948) Brittle fracture in mild steel plates. *Engineering* **165** 16.

[12] 12. Dulaney E.N. and Brace W.F. (1960) Velocity Behavior of a Growing Crack *Journ. of Applied Physics* **31** 2233.

[13] 13. Runde K. (1994) Dynamic instability in crack propagation. *Phys. Rev. E* **49** 2597.

[14] 14. Fineberg J., Gross S.P.,Marder M. & Swinney H.L. (1992) Instability in the propagation of fast cracks. *Phys. Rev. B* **45** 5146.

[15] 15. Gross S.P., Fineberg J., McCormick W.D., Marder M. & Swinney H.L. (1993) Acoustic emissions in dynamic fracture. *Phys. Rev. Lett.* **71** 1993.

[16] 16. Gross S.P. (1995), PhD. Thesis, Dynamics of Fast Fracture.

[17] 17. Sharon E., Gross P.G. & Fineberg J. (1995) Local branching as a mechanism in dynamic fracture. *Phys. Rev. Lett.* **74** 5096.

[18] 18. Sharon E., Gross P.G. & Fineberg J. (1996) Energy dissipation in dynamic fracture. *Phys. Rev. Lett.* **76** 2017.

[19] 19. Boudet J.F, CIliberto S. & Steinberg V. (1995) Experimental Study of the Instability of Crack Propagation in Brittle Materials, in *Europhysics Letters,* **30** (6), p.337.

[20] 20. Boudet J.F., Ciliberto S. & Steinberg V. (1996) Dynamics of Crack Propagation in Brittle Materials, in *Journal de Physique II,* **6**, p.1493.

[21] 21. Boudet J.F. & Ciliberto S. (1998) Interaction of Sound with Fast Crack Propagation, in *Physical Review Letters,* **81** p. 3546.

[22] 22. Green A.K. & Pratt P.L. (1974) Measurement of dynamic fracture roughness of PMMA by high-speed photography. *Eng. Fracture Mech.* **6** 71.

[23] 23. Kerkhof F. (1957) Ultrasonic fractography. Dans *Proceedings Third Internat. Congress High-Speed Photography,* Butterworths, London, p. 194.

[24] 24. Morrisey J.W. & Rice J.R. (1998) Crack Front Waves. *J. Mech. Phys. Solids*, **46**, 467-488 and private communication.

[25] 25. Griffith A.A (1920) The phenomena of rupture and flow in solids. *Phil. Trans. Roy. Soc. Lond.* **A221** 163.

[26] 26. Stroh A.N. (1960) A simple model of propagating crack. *Adv. Physics* **6** 418.

[27] 27. Carlsson J., L. Dahlberg & Nilsson F. (1973) Dynamic Crack Propagation. G.C. Sih, Leyden, Noordhoff.

[28] 28. Yoffe E.H. (1951) The moving crack. *Phil. Mag.* **42** 739.

[29] 29. Atkinson C. & Eshelby J.D. (1968) The flow of energy into the tip of a moving crack. *Int. J. of Material Sci.* **4** 3.

[30] 30. M. Adda-Bedia, *private communication.*

[31] 31. Barenblatt, G. I. (1959) The formation of equilibrium cracks during brittle fracture: The stability of isolated cracks, relationship with energetic theories. *Applied Mathematics and Mechanics* **23** 622-636.

8 Appendix : about the velocity instability threshold

In the following section, we want to develop a simple idea about the velocity instability threshold. In the first paragraph, we want to explain why we think that there is a possible acoustic origin for this threshold. After, we would explain this idea in more details.

Arguments for an acoustic origin of the velocity instability threshold : The main ideas are the following :

1) The experimental data about the oscillation frequency f give the following informations :

- f decreases with the thickness, but we don't have enough accuracy to characterize this decrease.
- The velocity oscillations frequency and the roughness oscillations frequency are not correlated [20].

2) The threshold does not depend on the thickness. Moreover, it has the same value in PMMA and in glass [14] : $V_{osc} = 0.33 V_R$.

These two experimental facts lead us to the following idea : to search a resonance between the crack front and a particular acoustic wave.

Description of the interaction : Consider the particular wave described in Fig.18. Consider that the crack front is a source of transverse acoustic waves. The waves propagate themselves in all directions. One of them emitted in A arrives at B at the same time that the crack front moving with a constant velocity V. In fact, this particular wave never leaves the crack front. We can evaluate the length h, defined in Fig.18, as function of the other parameters :

$$h = e \cdot \frac{V}{\sqrt{C_t^2 - V^2}}. \tag{52}$$

We consider here only the transverse waves for reasons that will be clarified below. Now, the following question is relevant : Under what conditions, this wave could be created ? We know that this wave is always on the crack front,

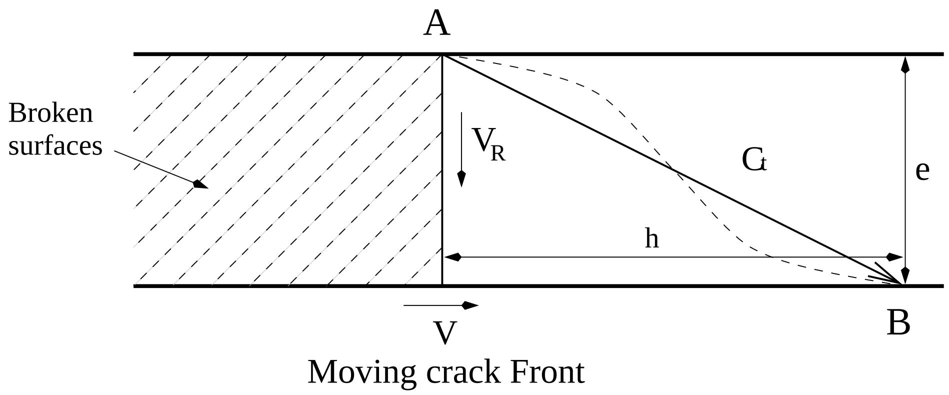

Figure 18: A scheme for the resonance between the crack front and an acoustic wave.

so the crack front can resonate only if the wave length λ_n is equal to $2e/n$ with n integer. λ_1 is equal to $2e$ and not e, because we want the wave phase to come back on itself. The velocity of this wave is naturally the Rayleigh wave speed, because this wave propagates itself along the broken surfaces. At the same time we have that the crack front is displaced by a length h at the velocity V. We can construct two typical frequencies $V_R/2e$ $(n = 1)$ and V/h: when h is a solution of Eq.52 both waves are simultaneously on the crack front. Thus there is a resonance. We can evaluate the characteristic velocity V_{osc} of the instability threshold, by identifying both frequencies: $\frac{V_R}{2e} = \frac{V}{h}$, where h is obtained from Eq.52. V_{osc} is then the solution of a Phytagoras theorem on the characteristic velocities of the problem:

$$C_t^2 = V_R^2 + V_{osc}^2. \tag{53}$$

This equation has no solution for $V < V_R$ when we consider the longitudinal waves instead the transverse waves. We have now a threshold of the instability appearance and a characteristic frequency equal to :

$$f_i = \frac{V_R}{2e}. \tag{54}$$

The predictions of this model are the following :

1) The value of the threshold depends only of the Rayleigh wave speed and Poisson's coefficient.

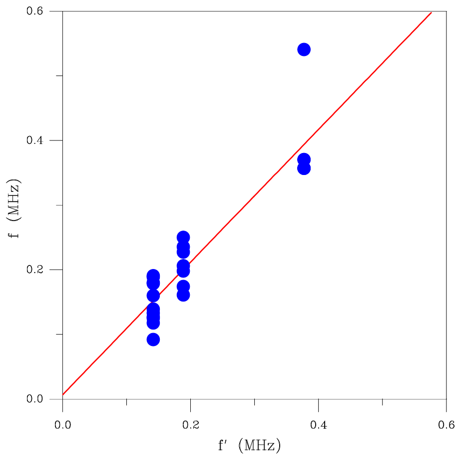

Figure 19: The frequency f as function of f'

2) The acoustic wave frequency decreases as $1/e$ and is equal to f_i. The value of f_i has to be corrected by the Doppler shift, since this acoustic wave is emitted by the moving crack tip. Therefore, the value of f_i measured in the laboratory frame is:

$$f' = \frac{V_R}{2e} \cdot \left(1 - \frac{V_{osc}}{C_t^d}\right). \tag{55}$$

These two predictions can be compared with the experimental results in glass and Plexiglass, which have the same Poisson coefficient $\nu = 0.33$. In agreement with the prediction, the threshold for acoustic emissions is the same in PMMA and glass. In Plexiglass we have also studied how the frequency of the waves, detected by one of the microphones, changes as function of e. In Fig.19 the measured frequency f is plotted as a function of f'. The line is a fit and the slope is equal to 1.02. The agreement is good, although error bars are very big.
Moreover, in glass, we only know that in samples of thickness equal to $3mm$, the typical frequency is 600 kHz [15], and the Rayleigh wave speed is three times bigger than in PMMA. Theoretically, this frequency must be equal to 500 kHz. There is again a good agreement.

Conclusions : We see that this simple model agrees with experimental results. We think that it is an idea which may prove to be fruitful. This model and the results are not a rigorous proof. However the agreement indicates, that this theoretical direction should be explored.